

Molecular Mechanism and Kinetics of Amyloid- β 42

Aggregate Formation: A Simulation Study

(SUPPORTING INFORMATION)

Viet Hoang Man,* Xibing He, Beihong Ji, Shuhan Liu, Xiang-Qun Xie, and Junmei Wang*

*Department of Pharmaceutical Sciences, School of Pharmacy, University of Pittsburgh,
Pittsburgh, PA 15213, USA*

E-mail: vhm3@pitt.edu; junmei.wang@pitt.edu

*To whom correspondence should be addressed

Definition of contact state and oligomers based on the mass center distance (r_{cen}) between two monomers.

The definition of contact state based on r_{cen} of two monomers is similar the one based on the minimum atomic distance (r_{min}) of two monomers, but r_{cen} was used instead r_{min} . Since it was reported that the gyration radius of A β 42 monomers could vary from 0.8 nm to 1.7 nm,¹⁻³ we use cutoff r_{cen} of 2.5 nm to define contact state of two monomers. It means two monomers will be in a contact state (dimer) when r_{cen} to be equal or smaller than 2.5 nm. The oligomers, which were defined by using this r_{cen} -based contact state definition, were named as r_{cen} -based oligomers.

Table S1: The solvent accessible surfac area (SA) of the A β 42 oligomers forming at different monomer concentrations.

| Oligomers | System | | | | | |
|-----------|------------------|------------------|------------------|------------------|------------------|------------------|
| | 20.13 mM | 13.42 mM | 9.44 mM | 6.85 mM | 3.91 mM | all systems |
| dimer | 32.61 \pm 1.84 | 32.33 \pm 1.67 | 31.97 \pm 1.90 | 31.28 \pm 1.86 | 31.84 \pm 1.68 | 31.83 \pm 1.76 |
| trimer1 | 31.97 \pm 1.52 | 31.34 \pm 1.40 | 30.66 \pm 1.47 | 31.04 \pm 1.24 | 30.53 \pm 1.50 | 30.74 \pm 1.48 |
| trimer2 | 30.24 \pm 1.48 | 29.83 \pm 1.36 | 29.16 \pm 1.50 | 29.20 \pm 1.40 | 29.12 \pm 1.24 | 29.23 \pm 1.37 |
| tetramer1 | 30.97 \pm 1.18 | 29.16 \pm 1.25 | 28.89 \pm 1.26 | 30.05 \pm 0.83 | 29.48 \pm 1.11 | 29.33 \pm 1.27 |
| tetramer2 | 30.03 \pm 1.16 | 30.39 \pm 1.46 | 30.70 \pm 0.82 | 30.91 \pm 0.89 | 30.21 \pm 0.96 | 30.40 \pm 1.13 |
| tetramer3 | 31.08 \pm 1.14 | 29.12 \pm 0.86 | 28.89 \pm 0.89 | 28.96 \pm 0.64 | 29.84 \pm 0.91 | 29.18 \pm 1.10 |
| tetramer4 | 28.79 \pm 1.35 | 28.99 \pm 1.26 | 28.54 \pm 1.07 | 28.63 \pm 1.29 | 28.42 \pm 1.20 | 28.73 \pm 1.26 |
| tetramer5 | 28.29 \pm 1.28 | 28.19 \pm 1.02 | 28.24 \pm 1.07 | 28.03 \pm 1.26 | 28.09 \pm 0.76 | 28.20 \pm 1.16 |
| tetramer6 | 27.79 \pm 1.13 | 27.29 \pm 0.91 | 27.39 \pm 1.02 | 27.11 \pm 1.11 | 28.08 \pm 0.53 | 27.38 \pm 1.06 |

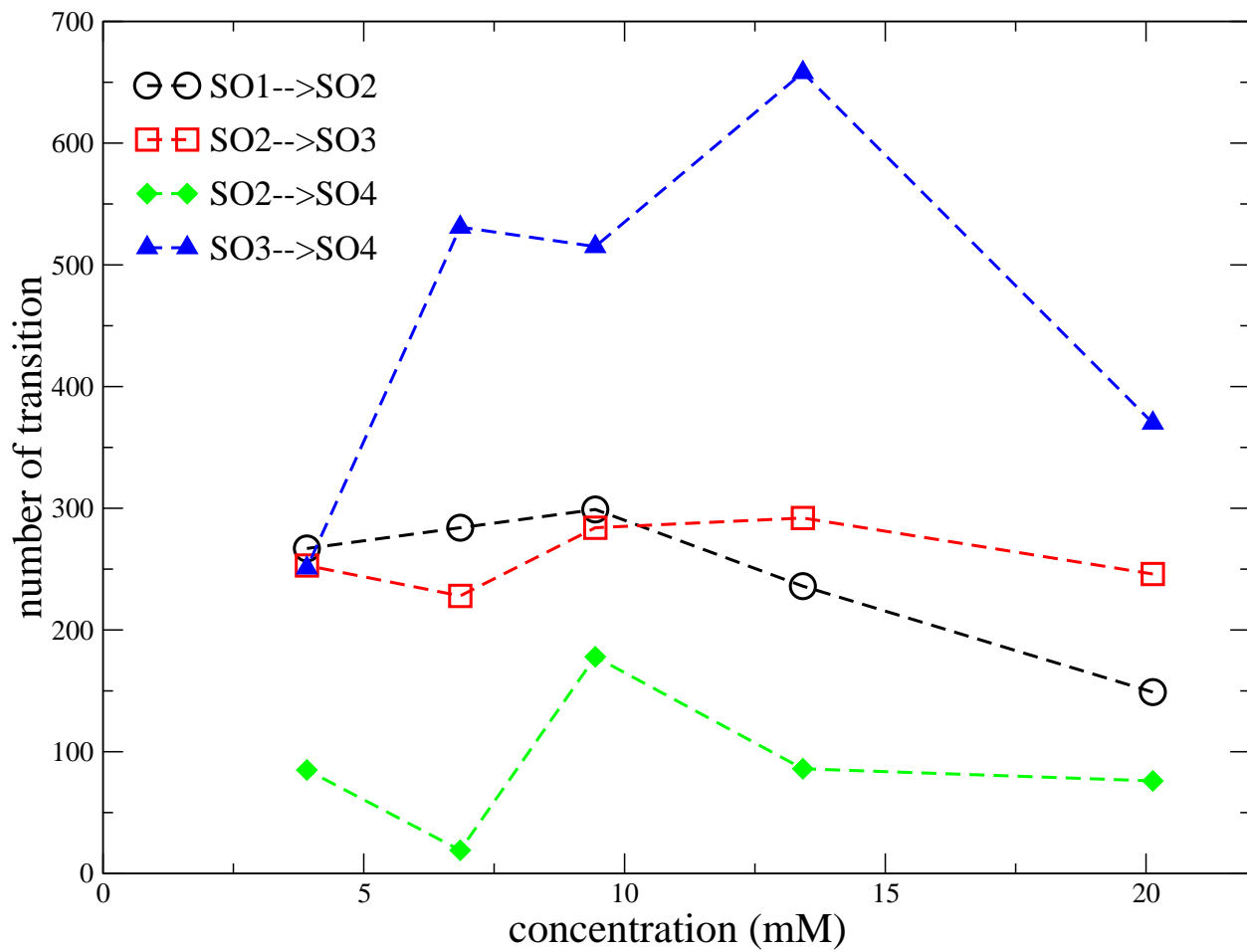


Figure S1: The dependence the number of $\text{SO}_i\text{-SO}_j$ transitions monomer concentrations of the $\text{A}\beta$ peptides. The data was calculated from all simulation systems and all the 500-ns simulation time of each MD run.

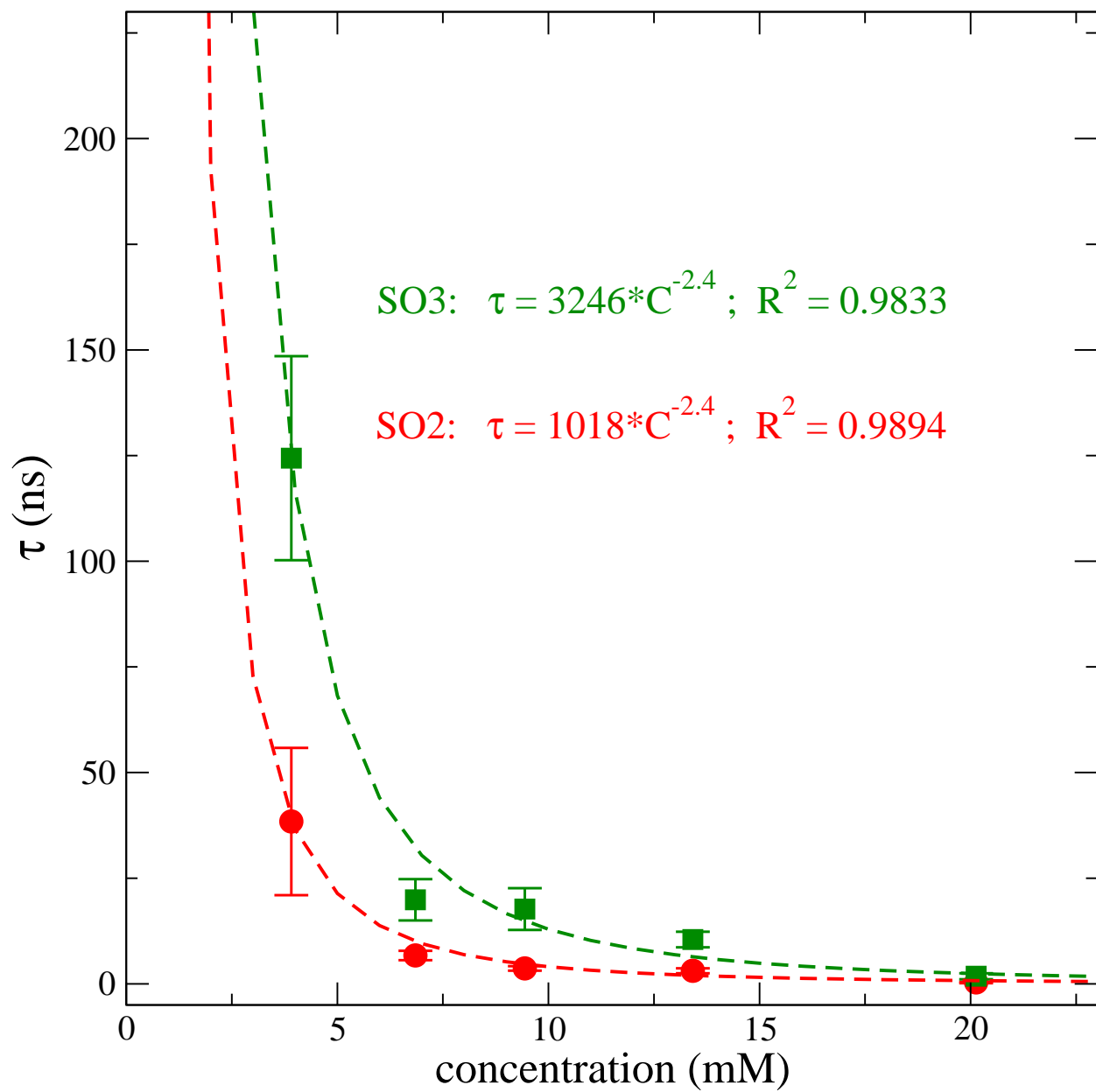


Figure S2: The dependence of the dimeric (red) and trimeric (green) oligomerization time (τ) on monomer concentrations of the A β peptides. The calculated data of the dimers and trimers are shown in red solid circles and green squares, respectively. The dash lines show the fitting data.

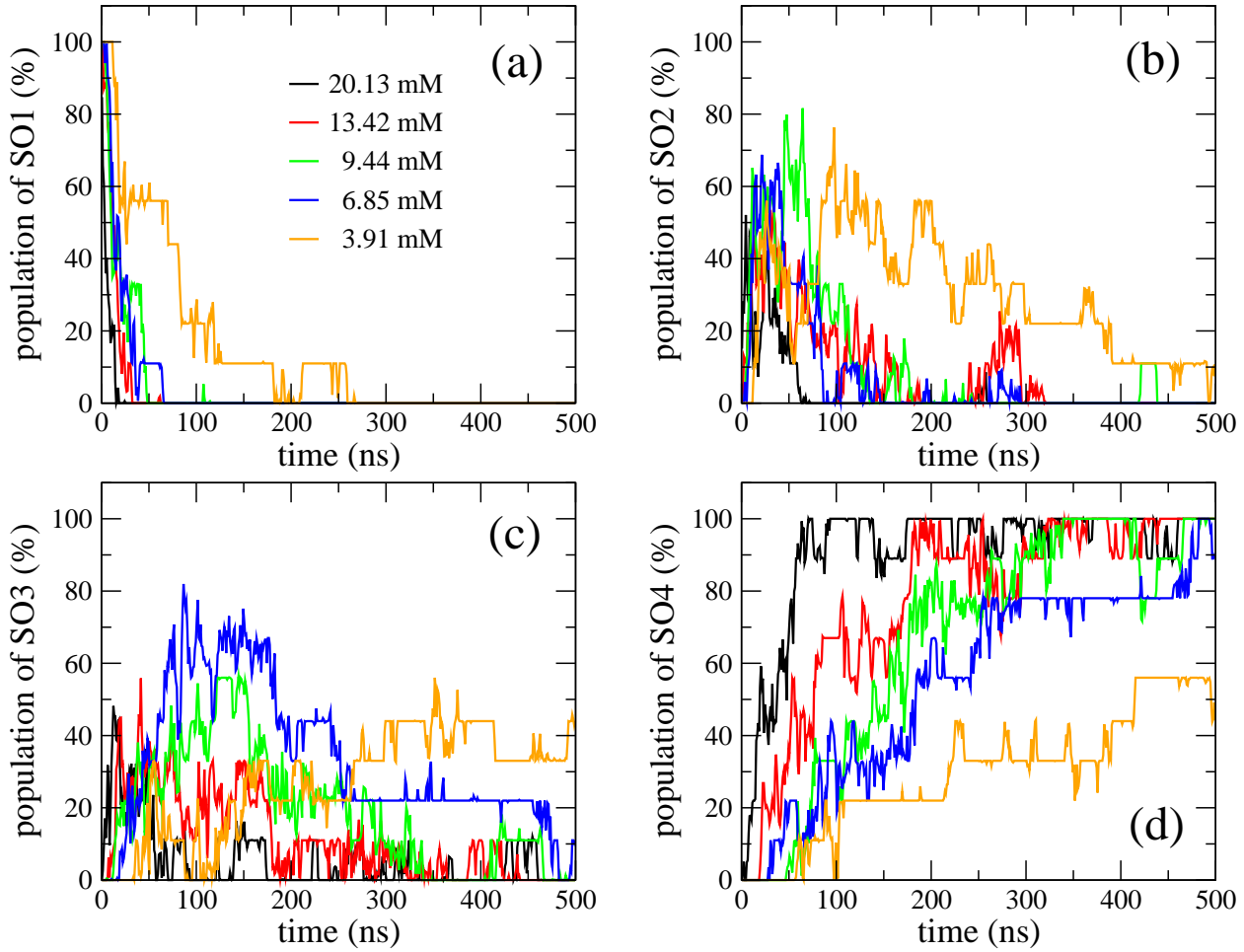


Figure S3: The evolution of the population of SO1, SO2, SO3 and SO4 states, which defined by using r_{cen} -based contact state definition (see above content), in the four-peptides systems are shown in (a), (b), (c) and (d) panels, respectively. The data were averaged from MD snapshots collected every 100 ps in all 9 MD runs for each concentration.

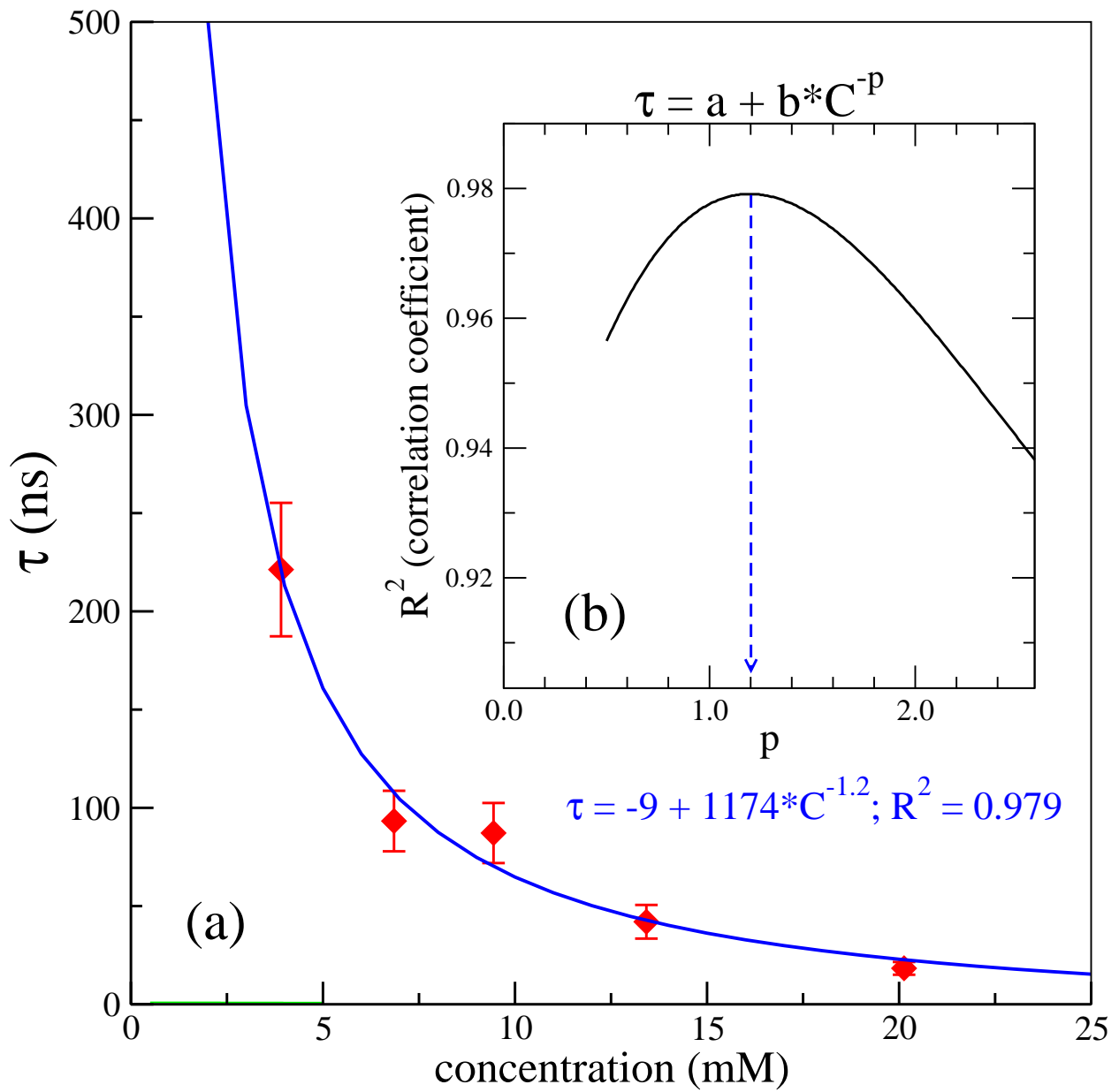


Figure S4: The dependence of the r_{cen} -based tetrameric oligomerization time (τ) on monomer concentrations of the $A\beta$ peptides. In panel (a), the red diamonds represent the data calculated from the simulations, while the blue line represents the best fit for the data. Panel (b) shows the dependence of the square of Pearson correlation coefficient (R^2) on the power (p) in the fitting by the non-linear function, $\tau = a + b * C^{-p}$, where a and b are constants and τ (in nanosecond) and C (in millimolar) are the oligomerization time and monomer concentration, respectively. The blue dash arrow points to the p value (1.2) which gives the maximum R^2 . The best fitting function is explicitly shown in blue text. The standard error was calculated from the 9 MD simulation trajectories for each state at each peptidic concentration.

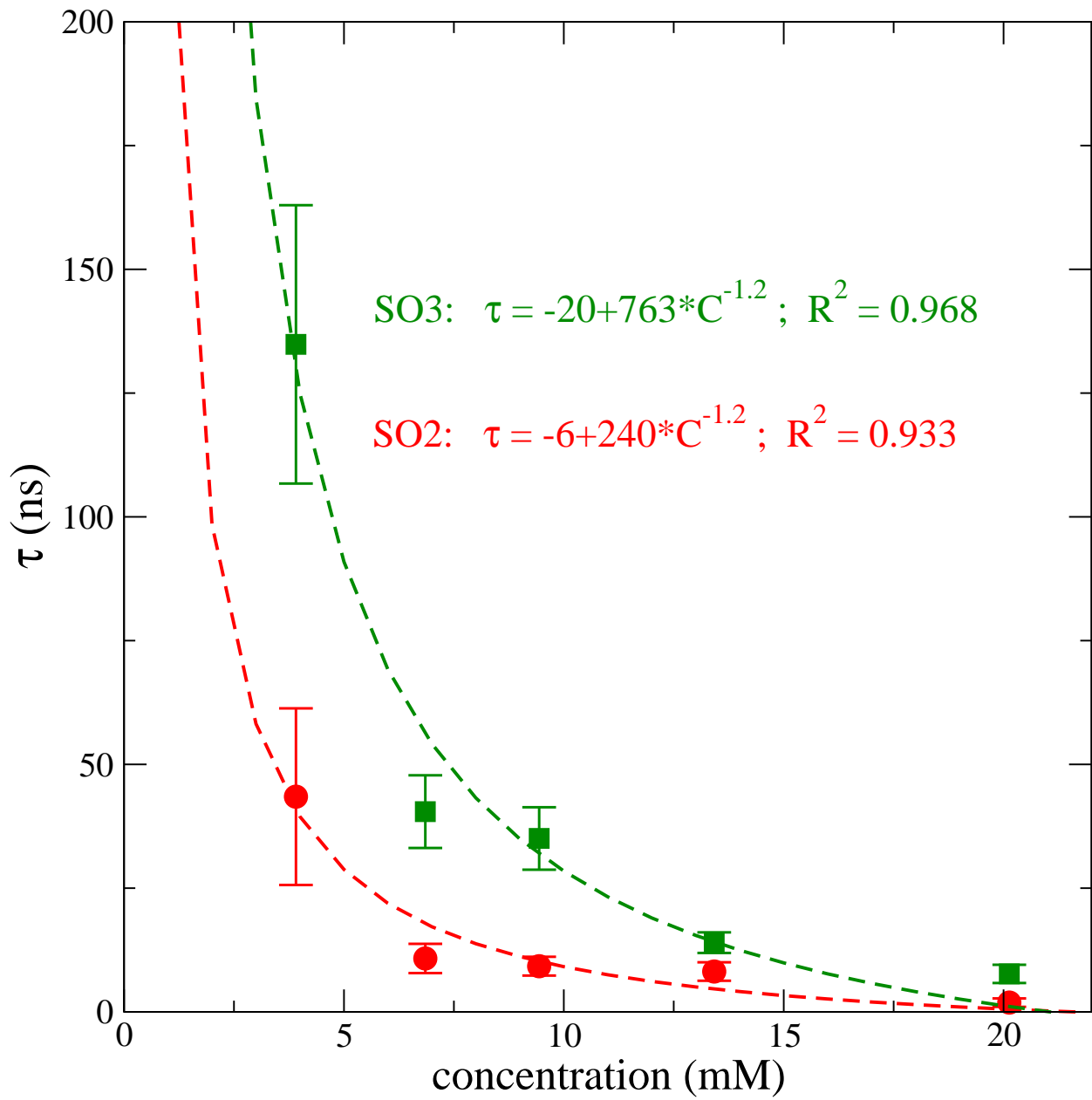


Figure S5: The dependence of the r_{cen} -based dimeric (red) and trimeric (green) oligomerization time (τ) on monomer concentrations of the A β peptides. The calculated data of the r_{cen} -based dimers and trimers are shown in red solid circles and green squares, respectively. The dash lines show the fitting data.

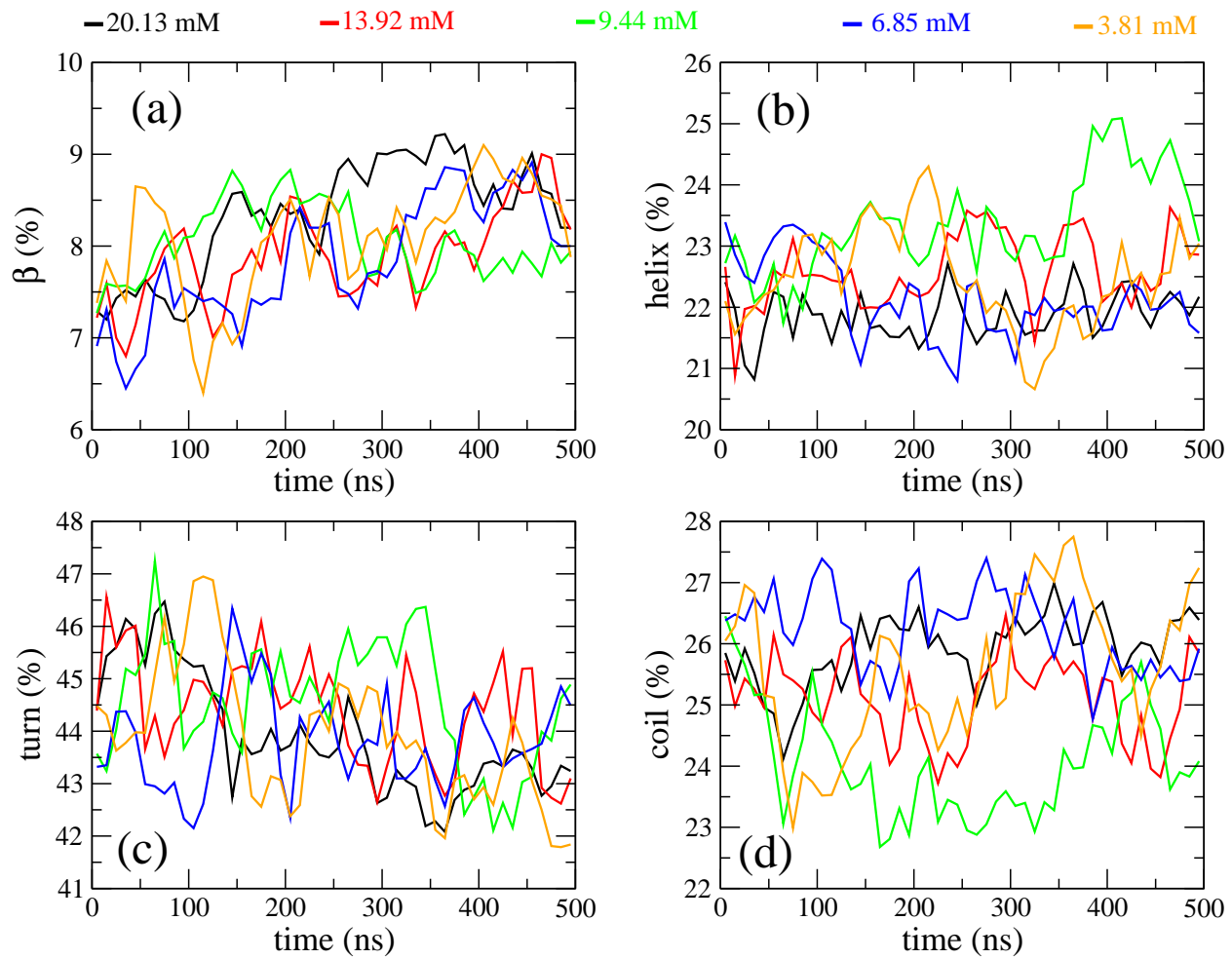


Figure S6: The time dependence of the secondary structures of A β 42 peptides in different systems, 20.13 mM (black), 13.92 mM (red), 9.44 mM (green), 6.86 mM (blue) and 3.81 mM (orange).

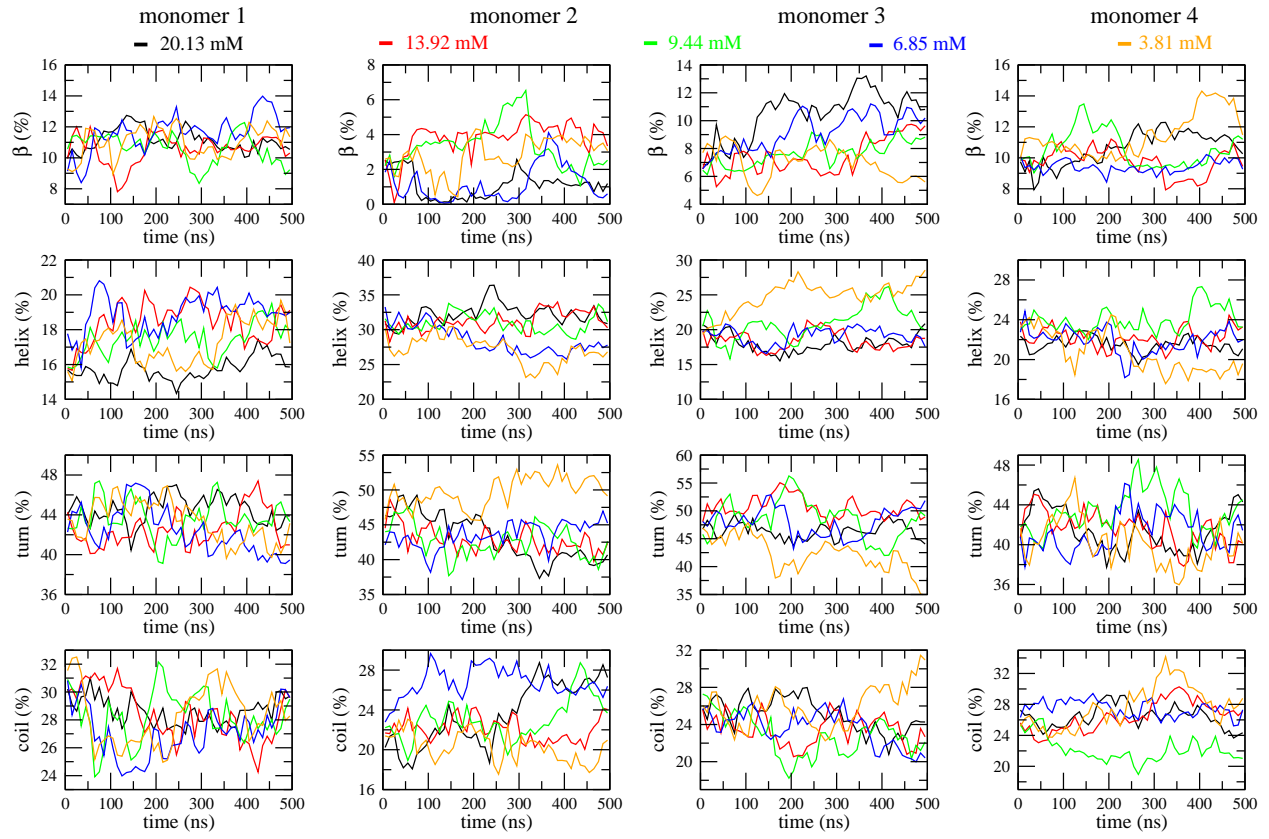


Figure S7: The time dependence of the secondary structures of individual monomers in different systems, 20.13 mM (black), 13.92 mM (red), 9.44 mM (green), 6.86 mM (blue) and 3.81 mM (orange).

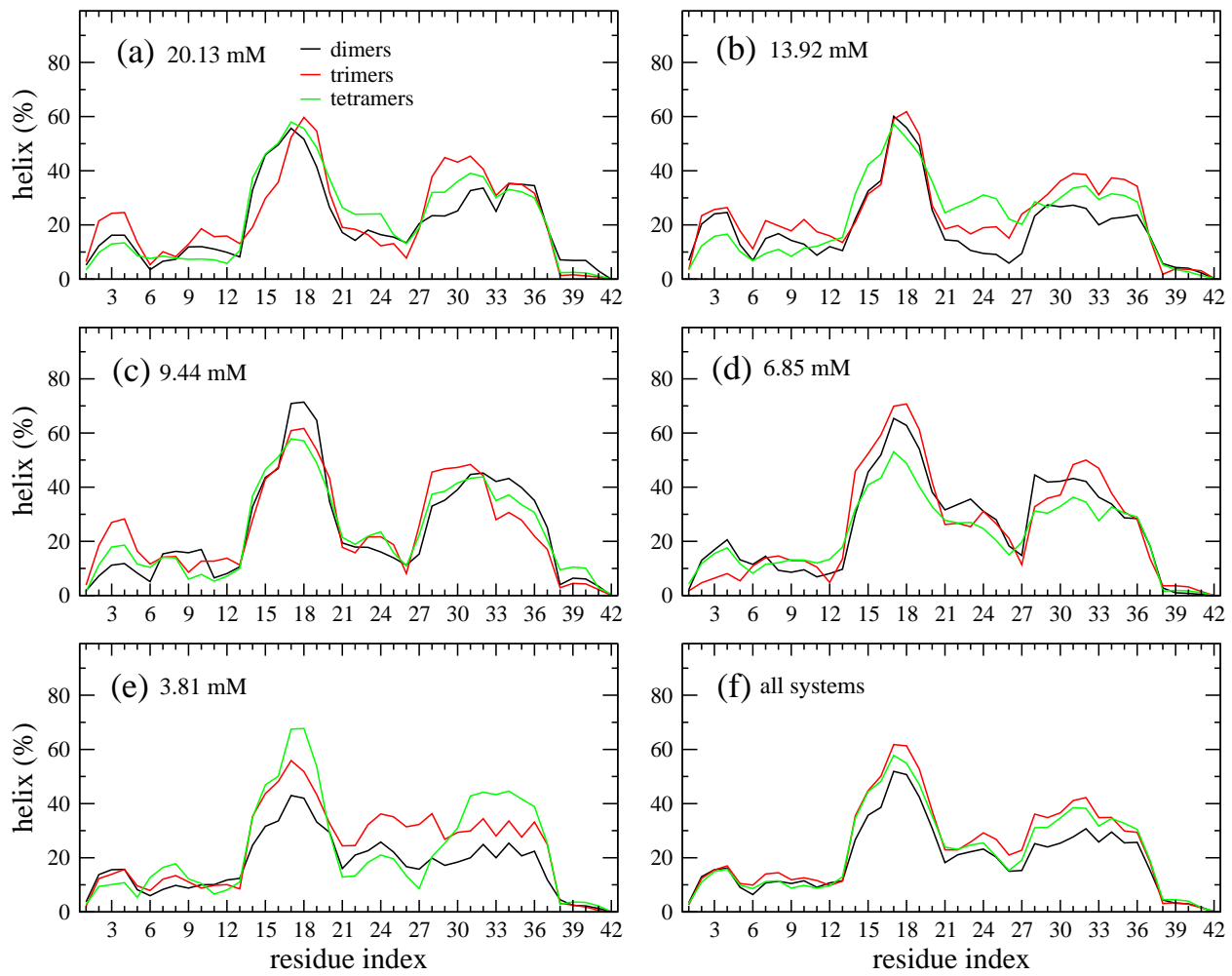


Figure S8: The helix propensities of each amino acid of A β 42 dimers (black), trimers (red) and tetramers (green) forming from different monomer concentrations, 20.13 mM (a), 13.92 mM (b), 9.44 mM (c), 6.85 mM (d) and 3.81 mM (e). Panel (f) is shown for the data calculated over all the considered monomer concentrations.

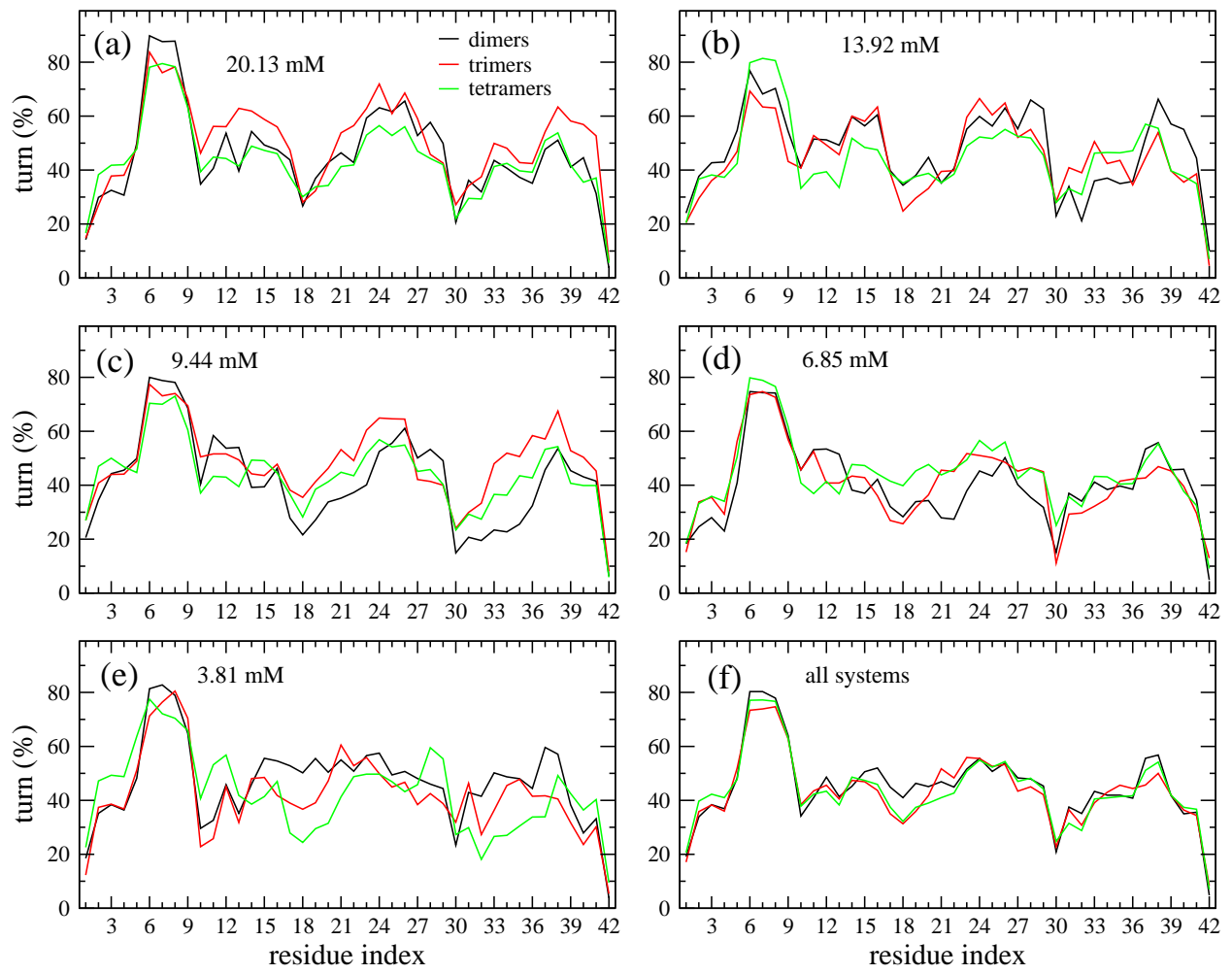


Figure S9: The turn propensities of each amino acid of A β 42 dimers (black), trimers (red) and tetramers (green) forming from different monomer concentrations, 20.13 mM (a), 13.92 mM (b), 9.44 mM (c), 6.85 mM (d) and 3.81 mM (e). Panel (f) is shown for the data calculated over all the considered monomer concentrations.

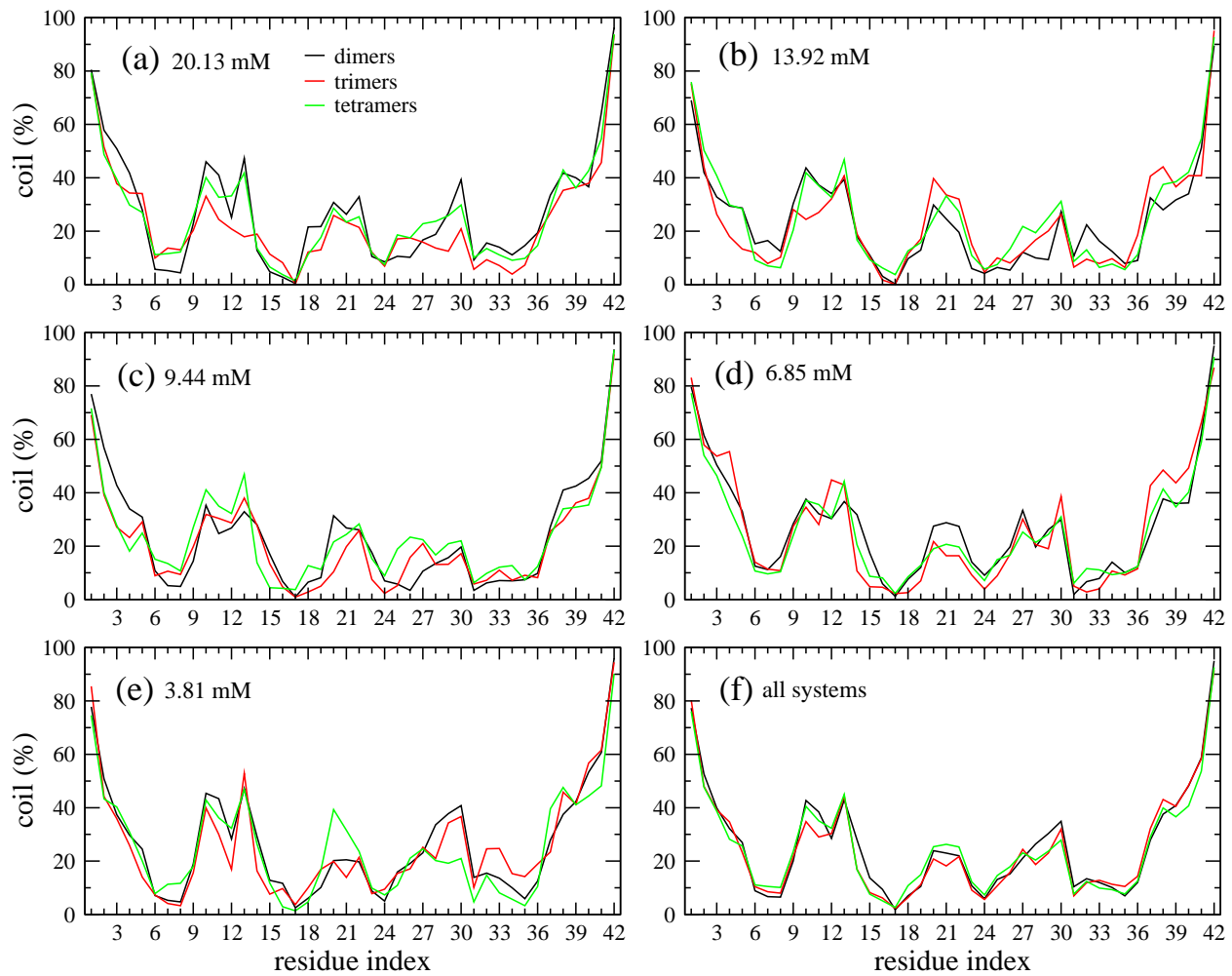


Figure S10: The coil propensities of each amino acid of A β 42 dimers (black), trimers (red) and tetramers (green) forming from different monomer concentrations, 20.13 mM (a), 13.92 mM (b), 9.44 mM (c), 6.85 mM (d) and 3.81 mM (e). Panel (f) is shown for the data calculated over all the considered monomer concentrations.

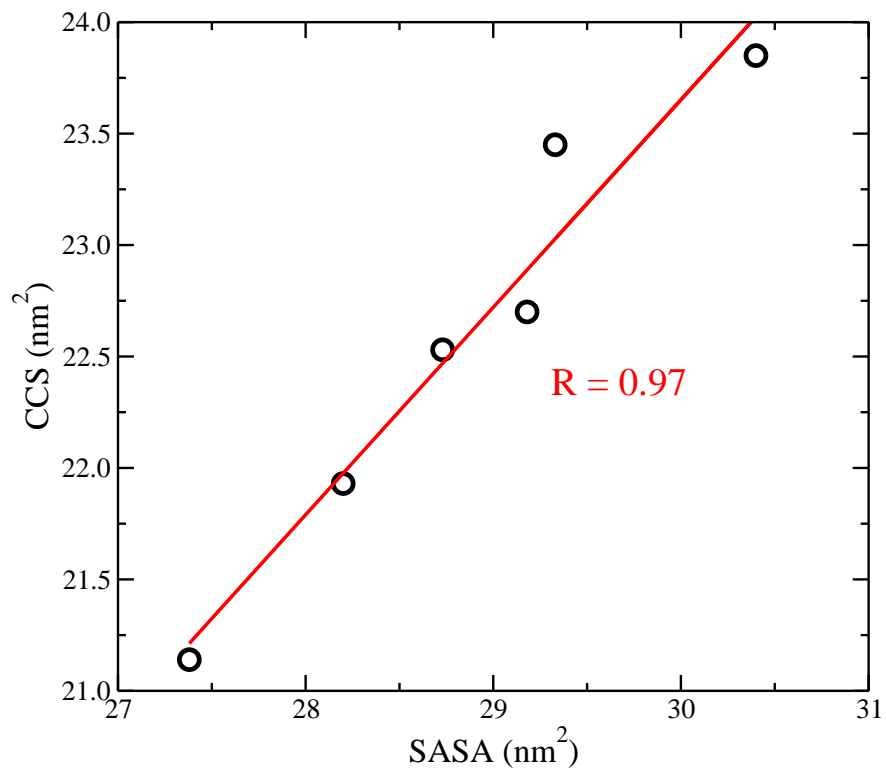


Figure S11: The correlation between CCS and SASA of the tetramers. The data of the six tetramer types is shown in black circles, while the fitting is red line. The Pearson correlation coefficient is 0.97.

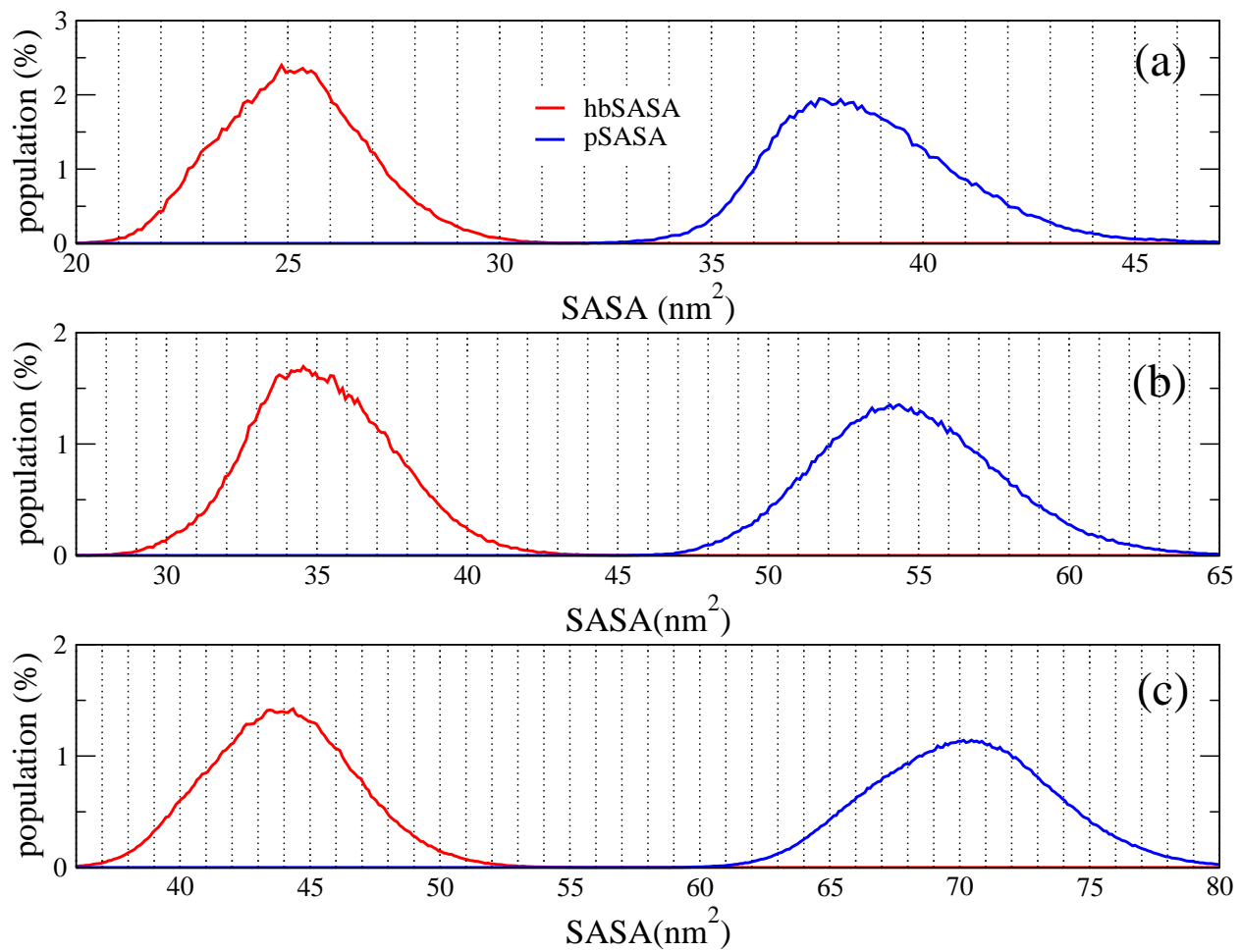


Figure S12: The hydrophobic solvent accessible surface area (hbSASA) and hydrophilic solvent accessible surface area (pSASA) distributions of the $\text{A}\beta 42$ dimer (a), trimer (b) and tetramer (c). The data was calculated from all simulation systems and all the 500-ns simulation time of each MD run.

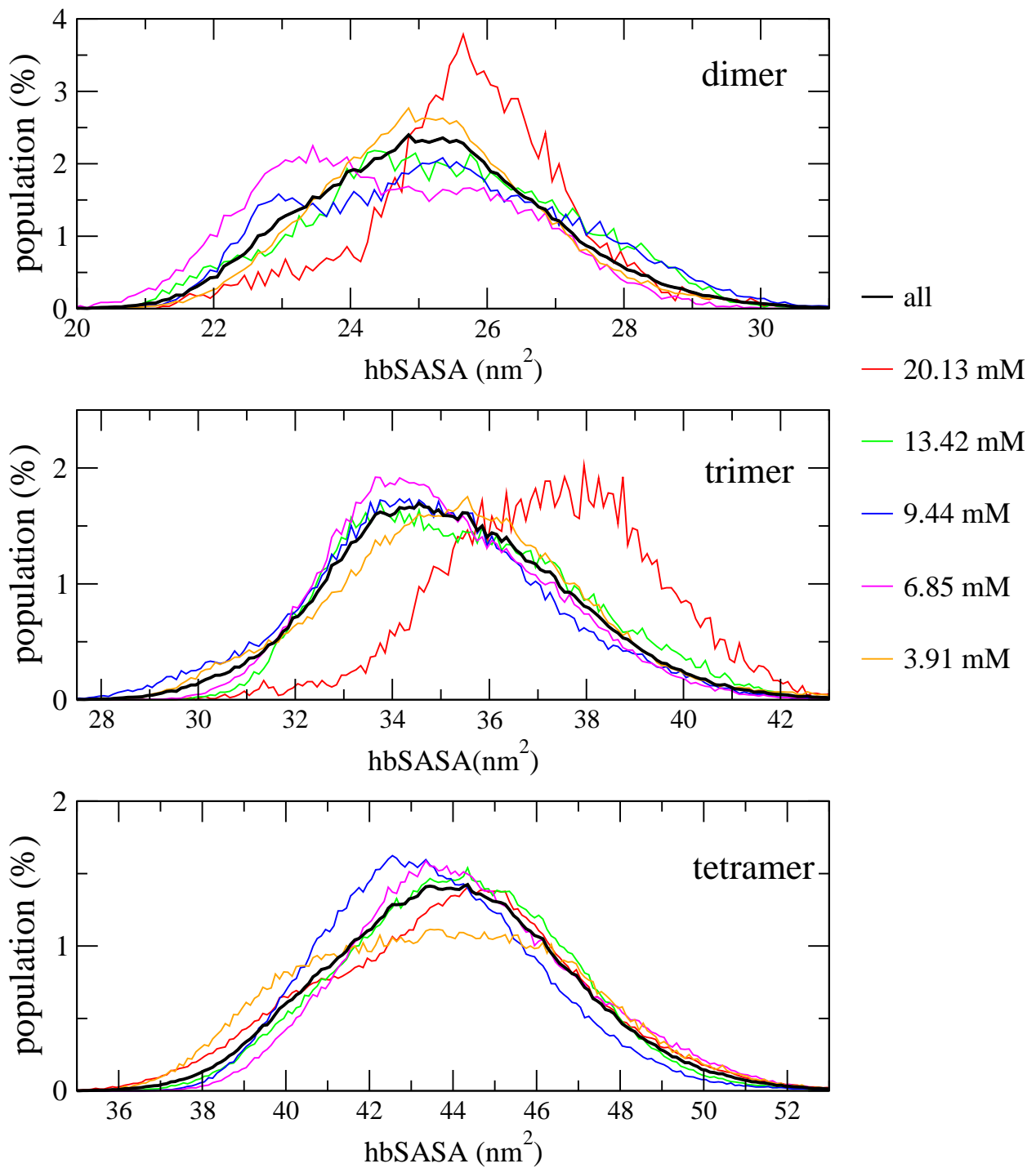


Figure S13: The hbSASA distributions of the Aβ42 dimer , trimer and tetramer forming at different monomer concentrations. The data was calculated from all simulation systems and all the 500-ns simulation time of each MD run.

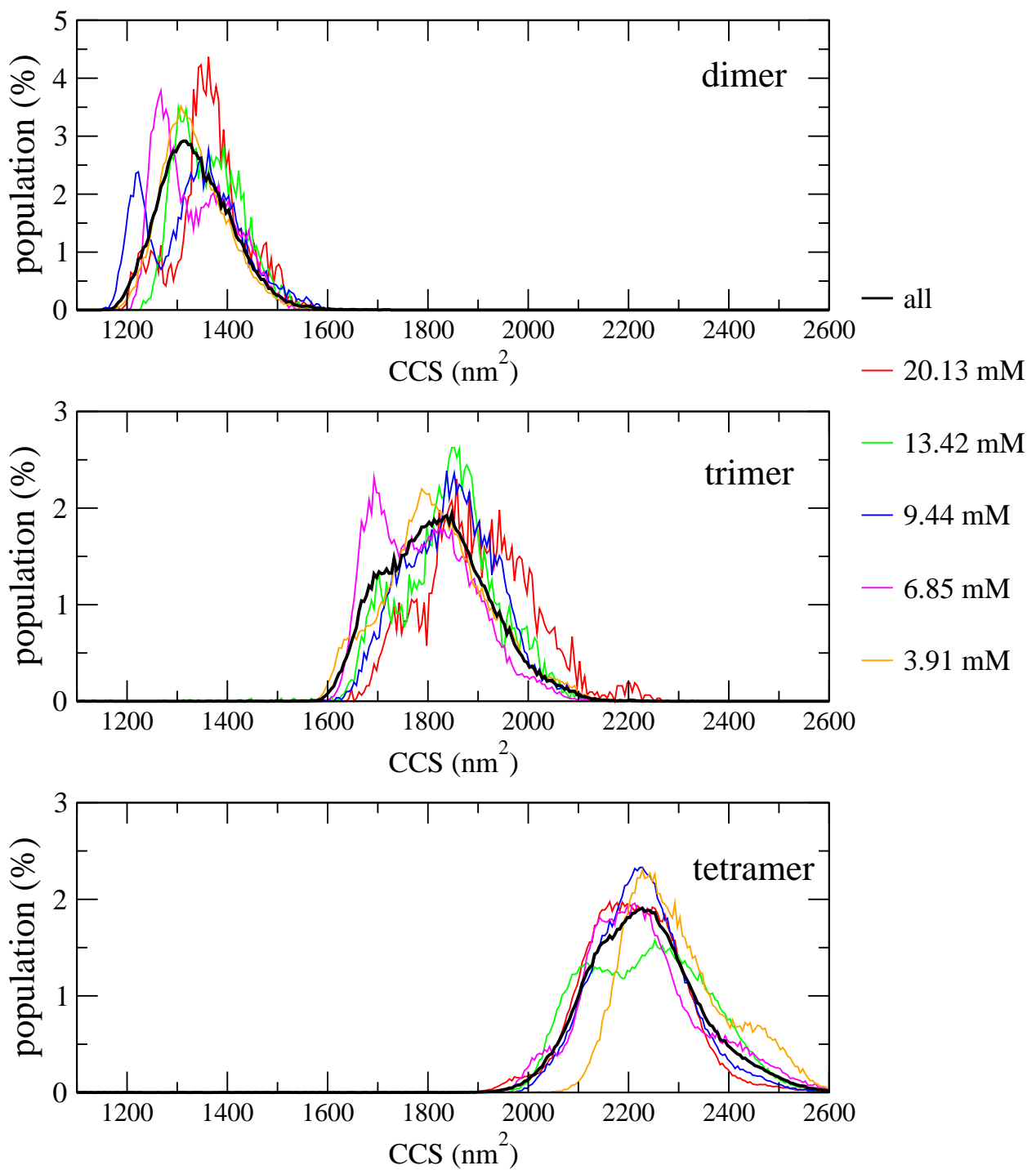


Figure S14: The CCS distributions of the A β 42 dimer , trimer and tetramer forming at different monomer concentrations. The data was calculated from all simulation systems and all the 500-ns simulation time of each MD run.

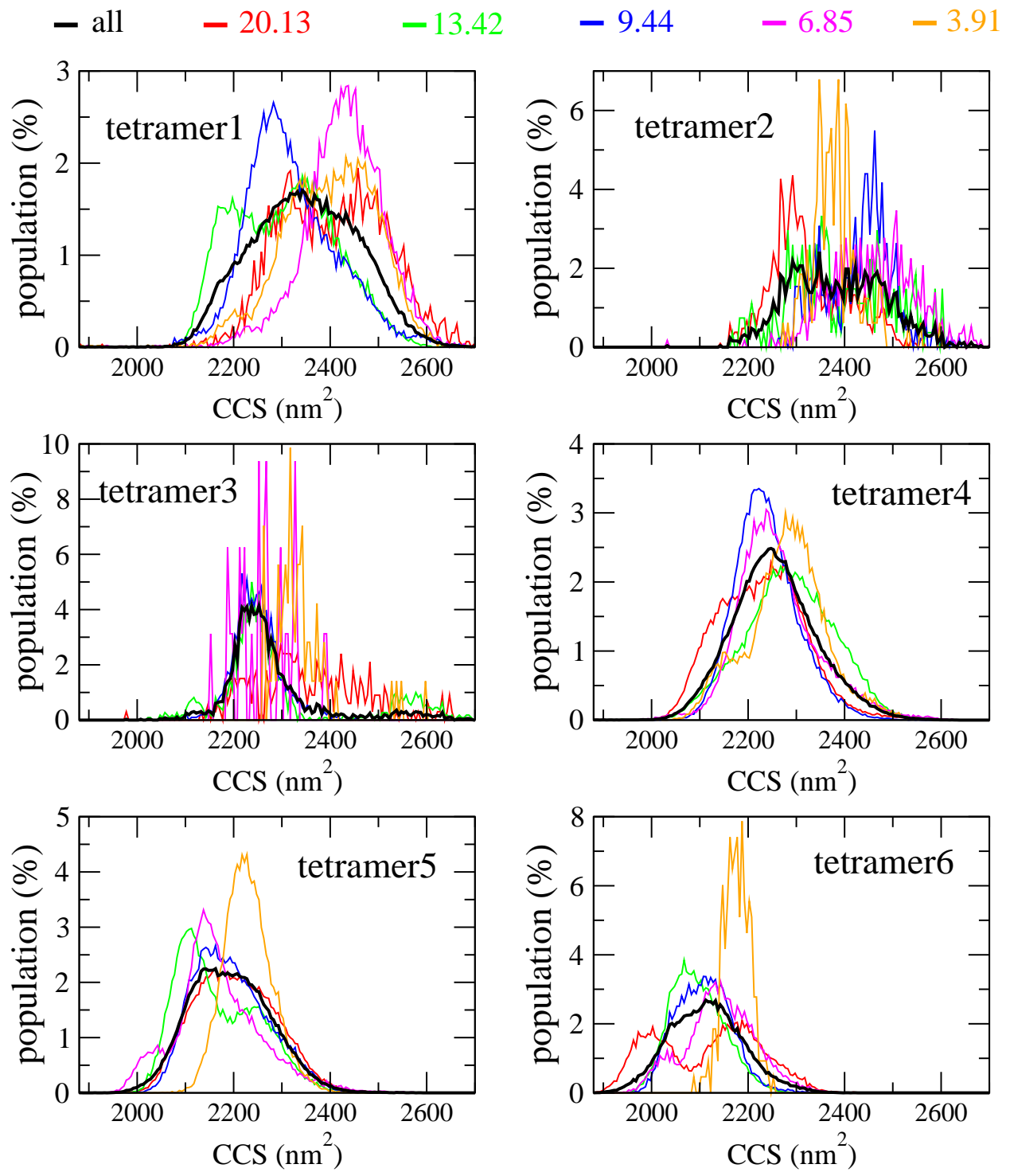


Figure S15: The CCS distribution of the tetramers. The data was calculated from all simulation systems and all the 500-ns simulation time of each MD run.

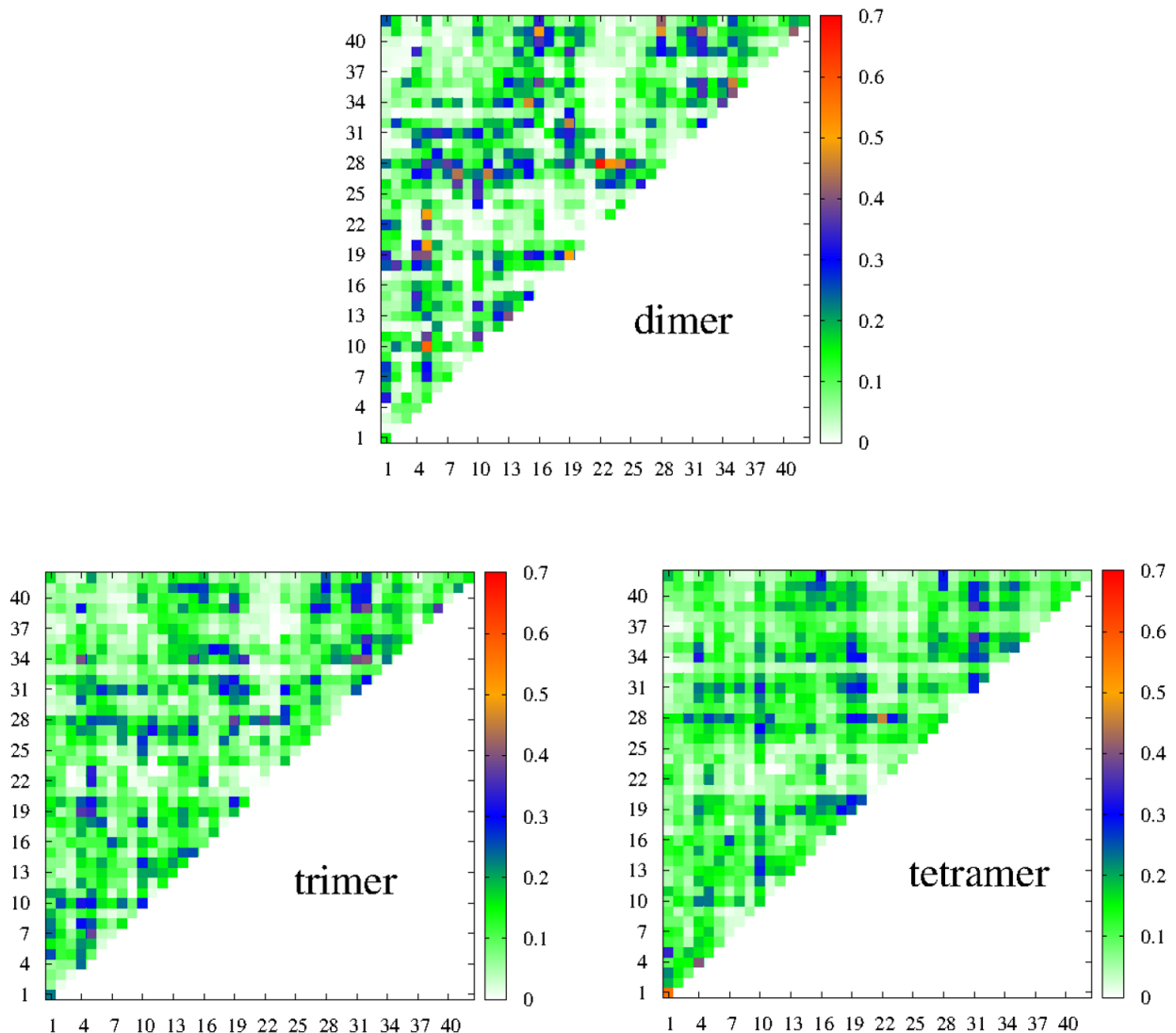


Figure S16: Intermolecular side chain-side chain contact probabilities (%) of A β 42 peptides in dimer, trimer and tetramer oligomers. The result are cumulated over all the concentrations.

Supporting References

- (1) Baumketner, A.; Bernstein, S. L.; Wyttenbach, T.; Bitan, G.; Teplow, D. B.; Bowers, M. T.; Shea, J.-E. Amyloid β -protein monomer structure: A computational and experimental study. *Protein Sci.* **2006**, *15*, 420–428.
- (2) Man, V. H.; Nguyen, P. H.; Derreumaux, P. High-Resolution Structures of the Amyloid- β_{1-42} Dimers from the Comparison of Four Atomistic Force Fields. *J. Phys. Chem. B* **2017**, *121*, 5977–5987.
- (3) Krupa, P.; Huy, P. D. Q.; Li, M. S. Properties of monomeric A β 42 probed by different sampling methods and force fields: Role of energy components. *J. Chem. Phys.* **2019**, *151*, 055101.